

# K&C Science Report – Phase 2

## ALOS Image Mosaics for Wetland Mapping

*Bruce Chapman*

Jet Propulsion Laboratory, California Institute of Technology, [bruce.chapman@jpl.nasa.gov](mailto:bruce.chapman@jpl.nasa.gov)

*Kyle McDonald*

Jet Propulsion Laboratory, California Institute of Technology, [kyle.mcdonald@jpl.nasa.gov](mailto:kyle.mcdonald@jpl.nasa.gov)

*Laura Hess*

University of California, Santa Barbara, [laurahess@gmail.com](mailto:laurahess@gmail.com)

### *Abstract—*

**ALOS PALSAR, an orbiting L-band SAR launched by the Japanese Aerospace and Exploration Agency (JAXA) in 2006, has been pursuing a global observation strategy through its ALOS Kyoto and Carbon Initiative (ALOS KC) [6]. The objectives of the ALOS KC project, lead by JAXA, include systematic global scale acquisitions by ALOS PALSAR, and the production of products quantifying the geographic extent of forested, desert, and wetlands [2].**

**In this report, we will describe our activities during the ALOS KC phase 2. The objective is the accurate ortho-rectification and calibration of ALOS PALSAR data for use in mapping inundated wetlands. We will describe data collected, calibration issues (both radiometric and geometric), ortho-rectification of the KC data, and completed mosaic products.**

*Index Terms—*ALOS PALSAR, K&C Initiative, Wetland Theme, Mosaic Theme, inundated wetlands

## I. INTRODUCTION

### *A. Science objectives*

A NASA funded research task will be generating an Earth Science Data Record for global inundated wetlands. Wetland extent and dynamics will be characterized using ALOS PALSAR imagery and other sensors. The extent and seasonal, inter-annual, and decadal variation of inundated wetland area play key roles in ecosystem dynamics. Wetlands

contribute approximately one fourth of the total methane annually emitted to the atmosphere and are identified as the primary contributor to inter-annual variations in the growth rate of atmospheric methane concentrations. Climate change is projected to have a pronounced effect on global wetlands through alterations in hydrologic regimes, with some changes already evident. In turn, climate-driven and anthropogenic changes to tropical and boreal peatlands have the potential to create significant feedbacks through release of large pools of soil carbon and effects on methanogenesis.

### *B. Ortho-rectification*

Ortho-rectification of the data consists of resampling the geocoded data into a well-known projection and file format. There are two reasons ortho-rectification of the PALSAR imagery is important for the development on an inundated wetlands product:

- 1) Field and validation data are geocoded. In order to make use of these data, the PALSAR image data must be accurately geocoded as well. Since inundated wetlands are highly variable and change at spatial scales comparable to the resolution of the PALSAR image data, the PALSAR image data must be geocoded to an accuracy commensurate to its pixel size. In order to easily verify the geocoding of the data, the data must be ortho-rectified.

- 2) SAR imagery is impacted by topographic slope. This terrain-induced change in backscatter can mimic the signature due to inundated wetlands

in areas where there should be no inundated wetlands (ie mountainous terrain). It is well known how to correct the radiometry of the image for this effect, but it requires that the imagery be well registered to the topographic data.

### C. Calibration

There are several types of calibration that must be applied to PALSAR image products.

1) Some image path products have processing artifacts present in the image. These processing artifacts can not be corrected and must be removed from the image.

2) The relative calibration of the image consists of evaluating and correcting for errors in the antenna pattern gain correction and, in the case for ScanSAR data, the removal of cross track banding at the seams of the different ScanSAR image beams.

3) The absolute calibration of the data consists of insuring that adjacent and overlapping paths of the ALOS image swaths have comparable image backscatter values. Adjacent and overlapping paths can have varying backscatter values due to both calibration errors and physical changes on the ground (ie. Change in moisture content). However, for the purposes of this task, the objective is the minimize these brightness variations, even if they are due to real physical changes to the landscape.

### D. Mosaicking

The last step is mosaicking image products. This step involves stitching together the ortho-rectified and calibrated image products. Evaluation of the image mosaic products is helpful for determining processing and acquisition gaps, and residual calibration errors, as well as being used for visualization of the data and product development.

## II. DESCRIPTION

### A. Relevance to the K&C drivers

The Wetlands theme of the ALOS KC initiative [2] will utilize ALOS image mosaics that have been ortho-rectified and projected to a simple ground projection. This simplifies quantitative analysis (i.e. overlap regions are eliminated) and validation and verification (i.e. it is easy to geographically compare with validation data sets). The mosaic theme of the ALOS KC initiative therefore enables this work by producing ortho-rectified image products. The

specific objective of this task within the ALOS KC phase 2 was to produce ortho-rectified ScanSAR imagery and mosaics in South America where rich multi-temporal image data will be acquired. Another objective of this was to continue the development of the dual polarization (HH/HV) ortho-rectified and calibrated image mosaic of North and South America.

The most basic requirement for modeling regional to global methane or carbon dioxide emissions from wetlands is a digital wetlands map with an appropriate scale and classification scheme [2]. The ultimate results of this project to map the extent and dynamics of inundated wetlands will therefore improve our understanding of the carbon cycle as well as facilitate conservation of wetland areas simply by identifying the location and maximum and minimum extent of wetlands.

### B. Work approach

The JAXA Earth Observation Research Centre (EORC) provides slant range “Path” image strips for use by the ALOS Kyoto and Carbon Initiative [2]. These image strips can be thousands of kilometers in length, but have a reduced resolution compared to that obtained during standard processing. The calibration is the same as that performed during standard processing, but the file format is slightly different.

The first step after path processing by the EORC is the ortho-rectification of the image data. For these results, we use the software package from Gamma Remote Sensing [7] to ortho-rectify the data to a supplied digital elevation model (DEM). The DEM data was constructed from the SRTM DEM, and other available DEM’s outside of the SRTM coverage area [8].

In order to organize and simplify the processing of the data, we use the UTM grid zones of the world (such as seen in [10]) to segment the world into sections measuring 6 deg of Longitude by 8 degrees of Latitude in size. Each path image is then ortho-rectified into each UTM grid zone that it passes through.

During KC phase 2, we discovered that the ScanSAR path products were difficult to geocode to the desired level of accuracy. Gamma Remote Sensing modified some code related to the

geocoding of ScanSAR KC path products, and subsequently, we found that the geometric accuracy could now be reliably assessed. However, we still found that, when compared to a simulated SAR image based on the SRTM DEM, there were still several pixel large errors in geolocation between the PALSAR data and the SRTM DEM. Meanwhile, pixel-level geolocation accuracy is critical for monitoring wetland dynamics.

In order to correct these geolocation errors, the Gamma Remote Sensing software includes software for estimating and correcting offsets between images. This software is designed to assist in co-registering pairs of SAR images prior to interfering them, but also can be used to correct the image geocoding parameters.

The wetland area in our study region in South America is a challenging one, as the imagery is very dynamic. The rivers and wetland areas change in appearance and sometimes slightly in location. However, we have found that cross-correlating the imagery against a simulated SAR image based on the SRTM DEM can be effectively used to determine geocoding errors, if the matching algorithm has robust parameters assigned to it.

After correcting any geocoding errors, the matching algorithm is again executed in order to produce an estimate of the effectiveness of the procedure. If the procedure is effective, the offsets should be less than 1 pixel. Figure 1 shows an example of the offset maps, in which the offsets in the slant plane of the path images in the range and azimuth direction are graphically visualized, before and after correction.

A procedure was implemented that successfully corrected any geocoding errors present in ScanSAR or fine beam path images. This procedure is applied separately for each UTM grid-zone that an image path crosses.

To examine the geometric errors present in the ScanSAR path images, we examined the mean range and azimuth offset from the SRTM DEM of 388 UTM grid-zone-projected images (see figure 2).

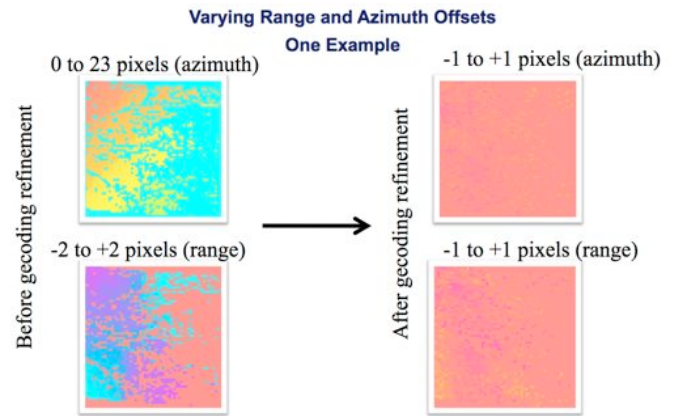


Figure 1: example of range and azimuth offsets for one UTM grid-zone projected path image, when compared with a simulated SAR image based on the SRTM DEM for the same region.

As can be seen, on average the range and azimuth offsets are very close to zero pixels, but it is not uncommon to see offsets greater than 1 pixel.

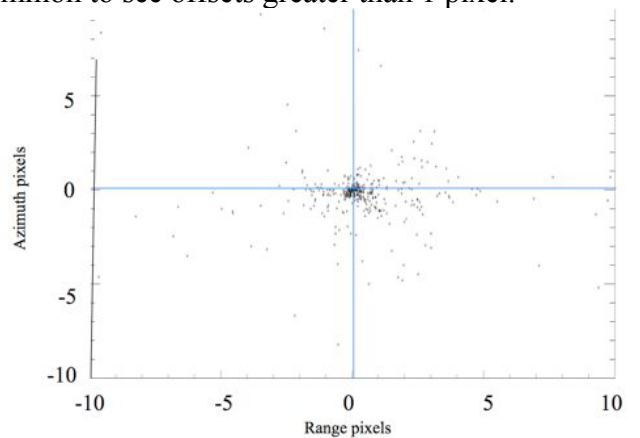


Figure 2: mean offsets of 388 UTM grid zone projected path images from SRTM DEM.

If we examine these offsets in more detail, we find that the mean range offset is -0.22 pixels in range, and -0.54 pixels in azimuth, with a standard deviation of over 4 pixels. If we exclude outliers from one RSP (424), in which the offsets were consistently greater than 10 pixels, we find that the mean range offset is 0.34 pixels, and the mean azimuth offset is -0.22 pixels, with a standard deviation of about 2 pixels. The range spacing for the EORC path images is 37.5 meters in range and 70 meters in azimuth, which leads to mean range offset of just  $12.8 \text{ m} \pm 82.5 \text{ m}$ , and a mean azimuth offset of  $-15.4 \text{ m} \pm 119 \text{ m}$  (excluding RSP424). However, even though the mean error is excellent, the variation about the mean necessitates estimating

and correcting geometric offsets for each path image.

Note that while the mean offset is quite small, as figure 1 indicates, the offset for each image is not a simple overall range and azimuth shift, but is a varying shift in both range and azimuth. To compensate for this variability, a 6<sup>th</sup> order polynomial was fit to the varying range and azimuth offsets and used to correct the varying shift for each UTM grid-zone-projected path image.

There are several approaches taken to correct for the various radiometric corrections.

First, each image path was trimmed in the near and far range, to insure that artifacts are not present in the final products (figure 3). Since there is, in general, ample overlap, this does not result in loss of much data. In fact, for ScanSAR data, the data in the near range is acquired at a very small incidence angle that is not very sensitive to backscatter signatures related to inundated wetlands, and should be discarded in any case.

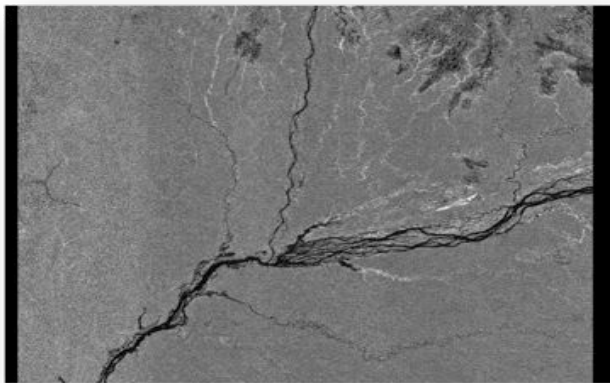
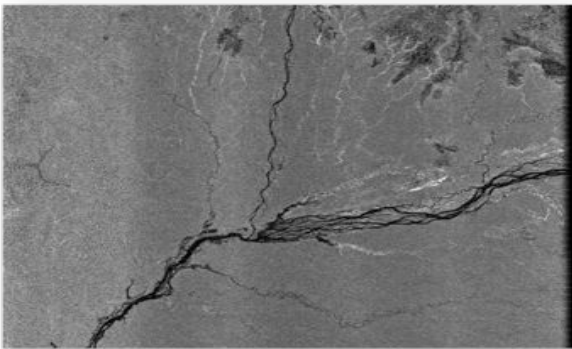


Figure 3. a) Original path image strip. b) Trim near and far range.

Secondly, some of the EORC path images that were processed early in the KC initiative, the

ScanSAR processing algorithm occasionally introduced banding in the ScanSAR path image strip that varied along track. This error can only be estimated empirically from the data. We also sometimes see an error similar to what a slight error in the antenna pattern correction could produce. We are still evaluating the best algorithm for correcting these and other similar range and azimuth dependent radiometric errors. In figure 4, dual polarized ALOS path imagery from an RSP over Alaska were averaged in the along track direction for the entire duration of the image strips. Then, the mean and standard deviation of the image brightness was determined for each range pixel. After averaging over more than a thousand kilometres, the resultant mean trend for each image strip would ideally represent the inverse of the required radiometric correction. As can be seen in figure 4, the nature of the trend for HH and HV are slightly different.

Currently, we have implemented an approach in which a large (~50km) running average of the average backscatter value (excluding both high and low backscatter values) is determined and the trend compensated.

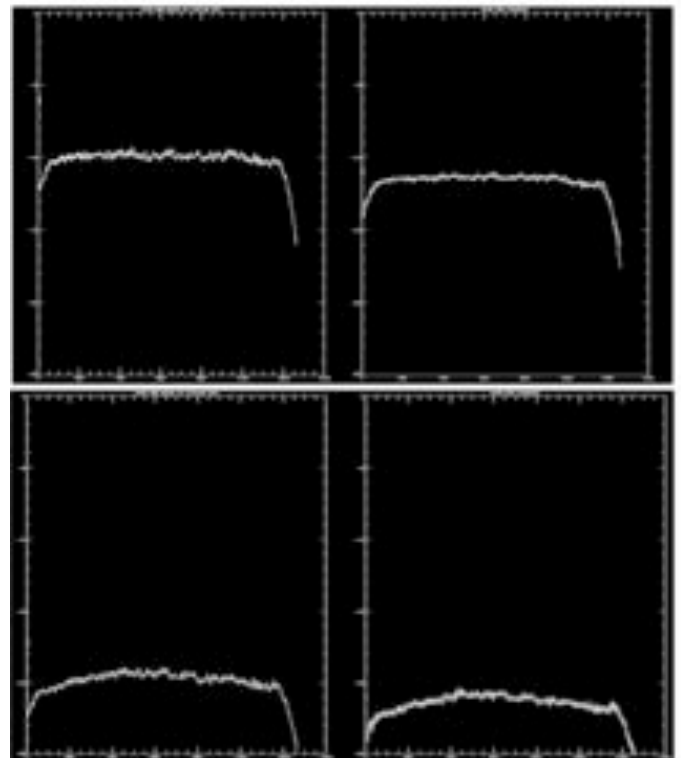
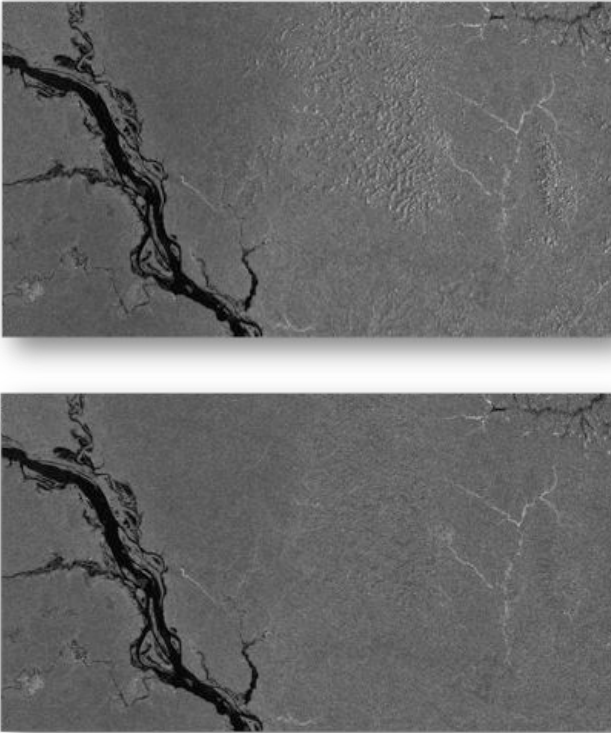


Figure 4. trends (before trimming) in the range direction. a) HH. b) HH, excluding data outside of 1db of mean. c) HV. d) HV, excluding data outside of 1db of mean.



**Figure 5. a) ortho-rectified imagery prior to radiometric terrain correction. B) ortho-rectified imagery after radiometric terrain correction. Without this correction, highland areas may have been improperly classified as inundated areas.**

Third, we use the Gamma Remote Sensing software to remove terrain effects introduced due to the changing pixel area illuminated within a pixel, due to topographic slopes (see figure 5). We perform this correction as these terrain-induced effects can introduce errors when trying to decipher the inundation state of the illuminated terrain, as terrain effects can mimic some of the signatures of inundation (low backscatter can imply open water, while high backscatter can imply inundated vegetation). However, this correction requires excellent geocoding, and an accurate knowledge of the topography at the pixel spacing of the ALOS imagery. For this purpose, in South America, we use the 3-arcsecond pixel-spacing SRTM DEM, which is comparable in resolution to the ALOS ScanSAR imagery. Outside of the SRTM coverage area, we use the best available DEM.

Stitching the ortho-rectified strips into a single image forms the mosaics. This stitching is done at JPL using JPL developed software called “multimosaic” [11]. There are several available options for this software related to deciding which

pixel from multiple images is preserved in the mosaic, if a single pixel is imaged more than once. When making single cycle mosaics, the option chosen was to have the far range portion of the imagery to take precedence over the near range imagery, if they overlap. Zero-fill areas are ignored.

Lastly, after a mosaic is constructed, it sometimes becomes visibly apparent that adjacent images have a significant difference in brightness. This manifests as a banding effect within the mosaic. This is an undesirable appearance, as it may result in the perception that there is a significant calibration problem with the data, as well as potentially making it problematic to correctly classify the status of inundation in wetland areas.

The image brightness may vary for a variety of reasons. The instrument calibration may be in error, or there may be processing errors at some stage. Since the radar backscatter of targets vary with incidence angle and with target type, and since ScanSAR data has a wide range of incidence angles within a swath (from 20 degrees to 50 or more degrees), some banding may be due to the varying nature of the scattering of whatever may be on the ground. Recent changes in moisture content of vegetation and/or ground soils can result in significant changes in backscatter as well (i.e. [12]). In the context of making it easier to identify locations of inundated wetlands, this change in brightness, whatever its cause, can be compared with adjacent images or an image average, and an empirical adjustment performed. This may, however, obscure physical signatures in the data. Changes in backscatter texture and contrast due to some of these effects, in particular those due to varying incidence angles within an image, cannot be easily corrected.

To examine this phenomena more fully, 70 ScanSAR image strips were analyzed from UTM grid-zone tile 19M in South America. For each pixel in tile 19M, the mean and standard deviation of the radiometrically corrected backscatter values were calculated, as well as the ratio of the standard deviation to the mean. If the ratio of the standard deviation to the mean was found to be less than 0.3 (which typically indicated that the pixel was not predominately open water or occasionally inundated vegetation), the mean difference between the mean

value and the individual value was determined. For these 70 ScanSAR image strips within tile 19M, millions of pixels satisfied this criteria. The mean mean-difference for each ScanSAR image strip was then calculated and plotted as a function of acquisition date, and the result is shown in figure 6.

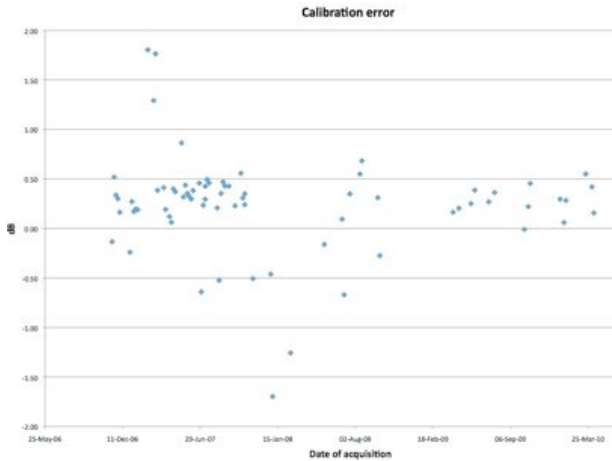


**Figure 6. Mean mean-difference between average image brightness and each of 70 ScanSAR image strips in UTM grid-zone tile 19M.**

As can be seen from figure 6, the mean difference typically varies less than 0.5 db, with occasional excursions of almost a couple of dB. Since the eye is sensitive to variations on the order of a tenth of a dB, without corrections, some of these variations of absolute brightness will be quite evident if not corrected.

Once the data is calibrated, it must be evaluated whether the calibration of the data, and the nature of the data itself, will allow for the identification of inundated wetland areas using the ALOS imagery alone. One simple wetland class that may be robustly identified in this ALOS ScanSAR imagery is open water when surrounded by a high biomass forest. Since the forest backscatter is high ( $\sigma^0 > -10\text{dB}$ ) the open water areas, which tend to have low backscatter values (except at small incidence angles), may be delineated with a simple threshold (values  $\sigma^0 < -10\text{dB}$ ). It is possible that areas of low vegetation could have similar backscatter values, depending on illumination incidence angle; therefore this must be validated prior to making definitive products. Figure 7 shows the application of this threshold to a mosaic of ScanSAR imagery, for a

location in Brazil along the Solimoes river.

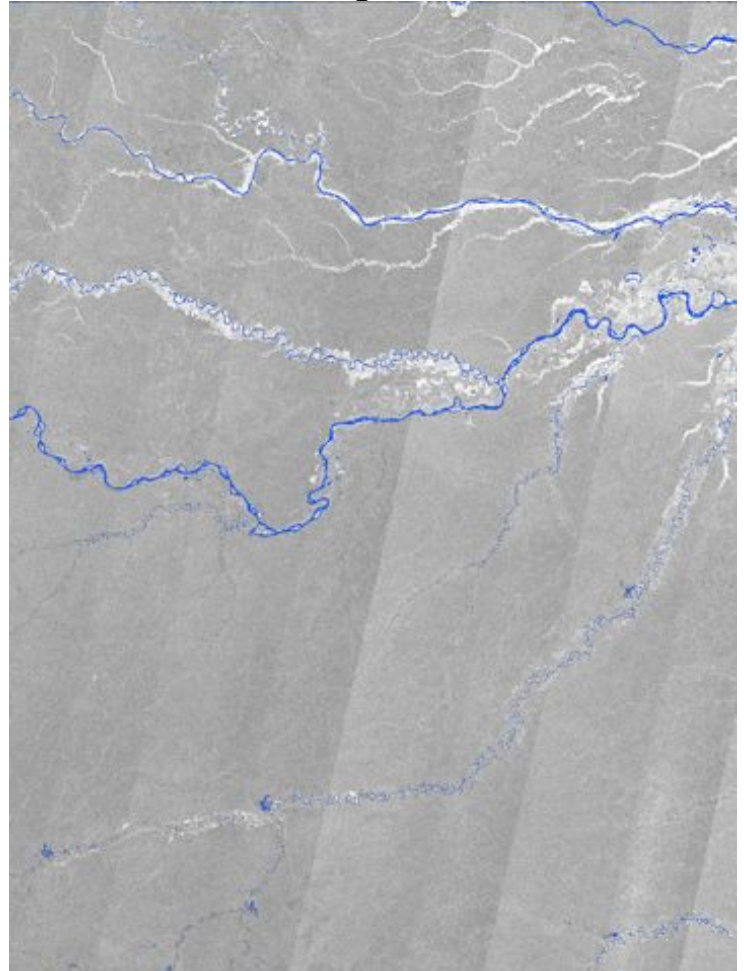


**Figure 7: Simple threshold ( $\sigma^0 < -10\text{dB}$ ) indicated in blue for identifying open water. Solimoes river, Brazil.**

Another simple wetland class that may be robustly identified are inundated vegetation areas. In this case, the inundated vegetation is much brighter than the surrounding non-inundated forests ( $\sigma^0 > -6\text{dB}$ ). Figure 8 shows an example of thresholding the data with this value. As can be seen, this threshold roughly identifies the location of inundated vegetation. However, there are other features, such as urban areas, that have similar backscatter values as inundated vegetation; therefore, this must be validated prior to making definitive products. However, this verifies that the ALOS ScanSAR data is both well enough calibrated and with high enough sensitivity to these inundation conditions to begin this work.

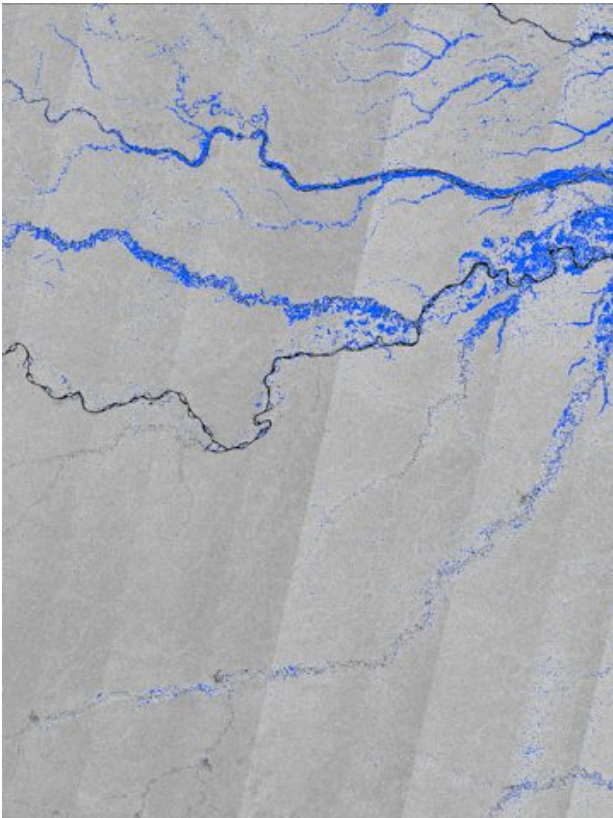


Figure 8: Simple threshold ( $\sigma^0 < -6\text{dB}$ ) indicated in blue for identifying inundated vegetation. Solimoes river, Brazil.

Many of the described processing steps are CPU intensive. In order to facilitate the processing of this data, in particular the ortho-rectification of the data, some processing has been conducted on “Pleiades” at the NASA Advanced Supercomputing Division located at the NASA Ames Research Center. Pleiades, in 2009 the sixth most powerful supercomputer in the world, represents NASA's state-of-the-art technology for meeting the agency's supercomputing requirements, enabling NASA scientists and engineers to conduct modeling and simulation for NASA missions. It consists of 148 computer racks holding 9,472 nodes with 84, 992 cores and a total memory of 133 TBytes.

### C. Satellite and ground data

The ortho-rectification of the dual polarization ALOS PALSAR data is dependent on the DEM reference used. For this work, the SRTM 90 DEM from CGIAR-CSI [8,9] was oversampled to one arc-second pixel spacing and padded to overlapping and padded DEM tiles. The ALOS dual polarization data and ScanSAR data are in the slant range

projection from the JAXA EORC, and span Summer 2007 to the end of 2010.

### III. RESULTS AND SUMMARY

Figure 9 shows a mosaic of the average of 221 ScanSAR path images from late 2006 to mid 2010, which have been subsetted into 1253 UTM grid-zone tiles. Typically, each pixel in this mosaic is an average of approximately 10 path image pixels, as governed by the location of each processed image. Each ScanSAR mosaic is posted with a pixels spacing of 3 arcseconds, or approximately 90 meters.

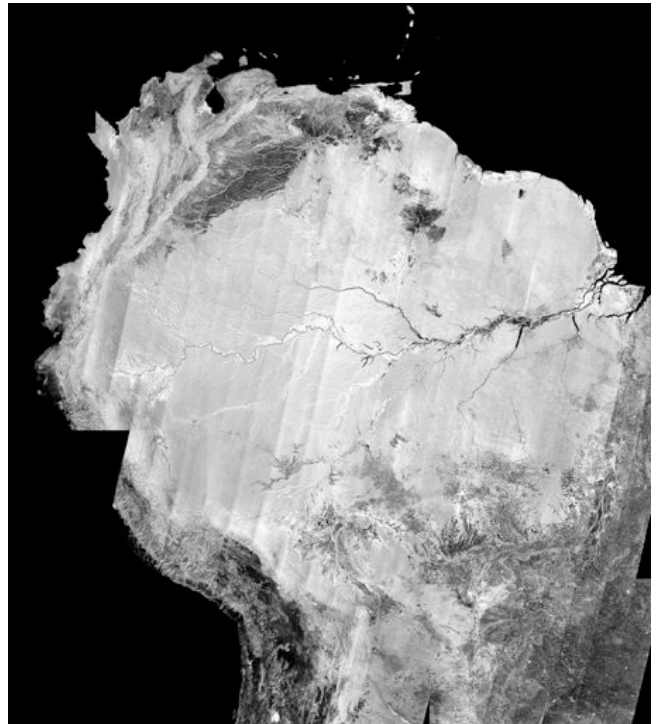
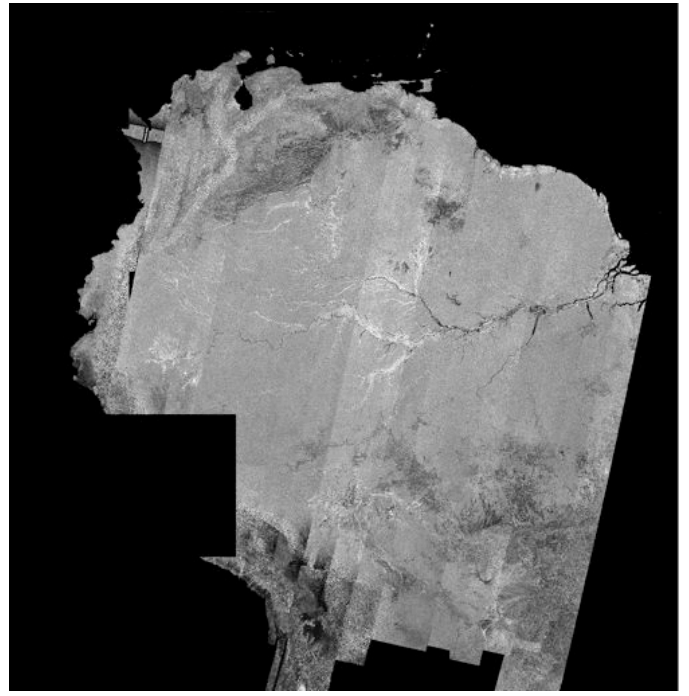


Figure 9. Mosaic of average of ScanSAR images (late 2006 to mid 2010).

In addition to an average image mosaic, figure 10 shows mosaics of ScanSAR data acquired within adjacent pairs of ALOS orbit cycles. Some cycles have better coverage than others due to the global observation scenario, acquisition conflicts, and available processing resources. Some path images and UTM grid-zone locations have not yet been ortho-rectified.



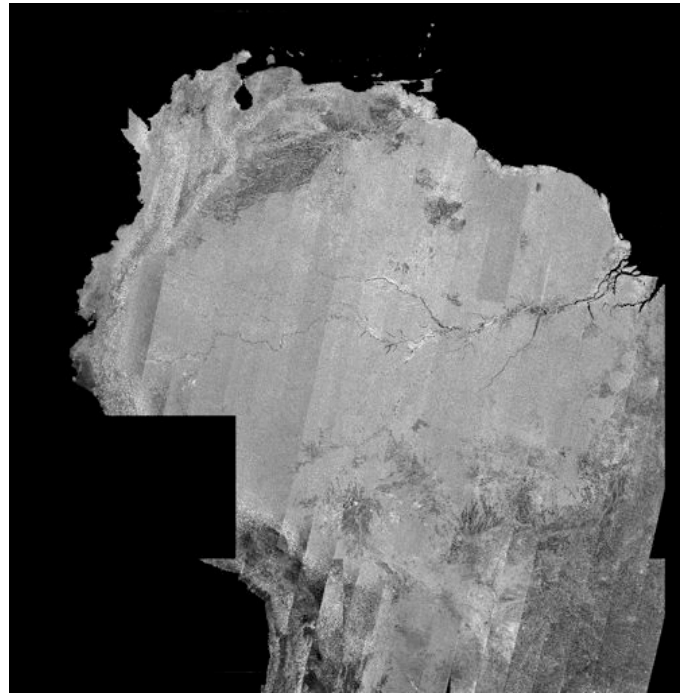
10a) ScanSAR mosaic of cycle 7 and cycle 8



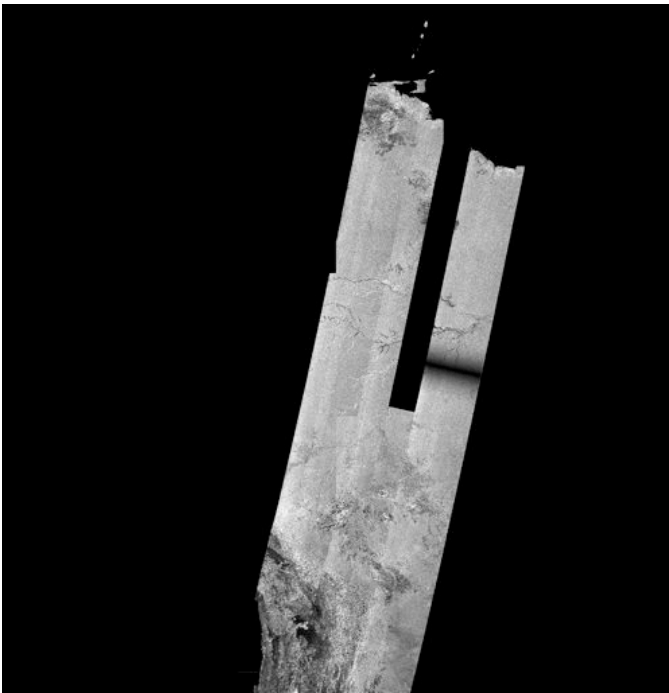
10c) ScanSAR mosaic of cycle 11 and cycle 12



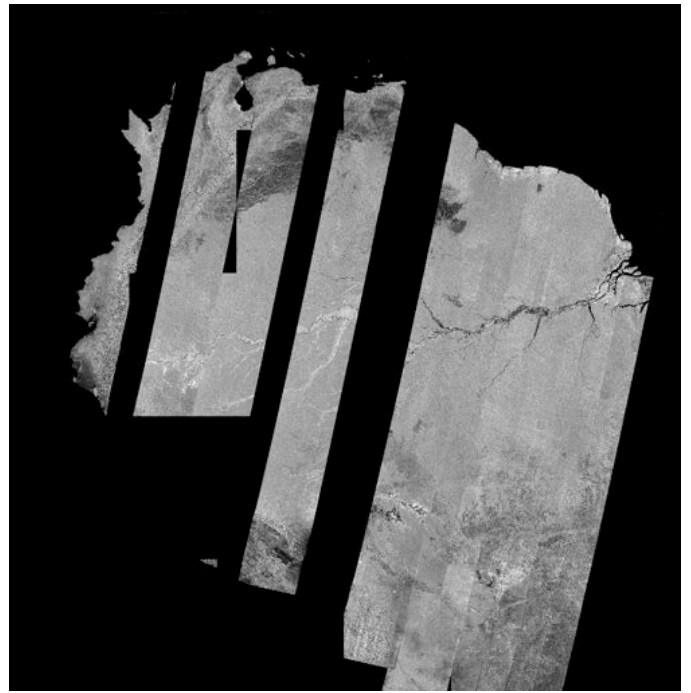
10b) ScanSAR mosaic of cycle 9 and cycle 10



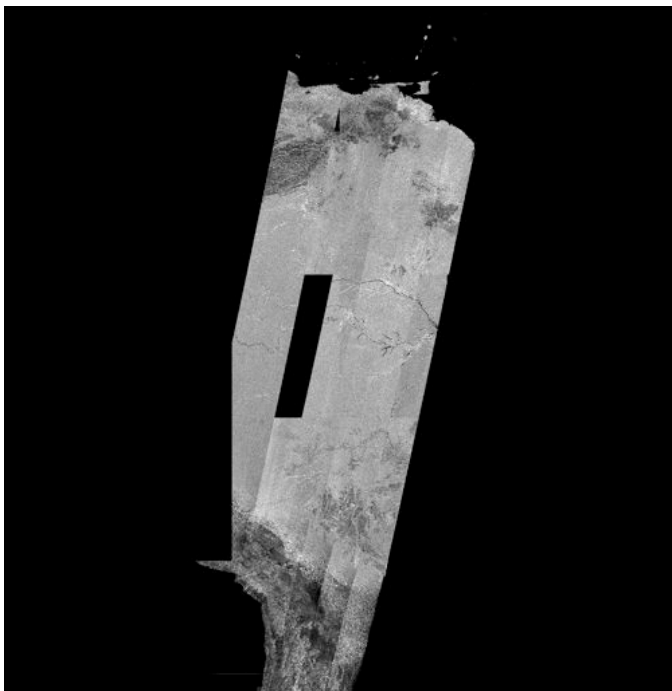
10d) ScanSAR mosaic of cycle 13 and cycle 14



10e) ScanSAR mosaic of cycle 15 and cycle 16



10g) ScanSAR mosaic of cycle 25 and cycle 26



10f) ScanSAR mosaic from cycle 17 to cycle 24



10h) ScanSAR mosaic of cycle 27 and cycle 28



10i) ScanSAR mosaic of cycle 29 and cycle 30



10k) ScanSAR mosaic of cycle 33 and cycle 34



10j) ScanSAR mosaic of cycle 31 and cycle 32

These continental scale mosaics are shown for localized locations to illustrate the data quality at full resolution. First, from the mosaic of the average of ScanSAR images: Figure 11 is the area near Noel Kempff National park, figure 12 is includes the Rio Branco, figure 13 is over an area in peru with large palm swamps, figure 14 shows the area near the Rio Negro, and figure 15 shows the Orinoco river delta.

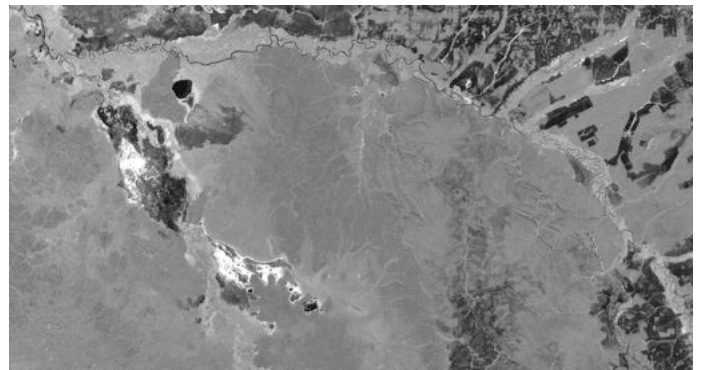


Figure 11: Noel Kempff National Park from mosaic of average of ScanSAR images.

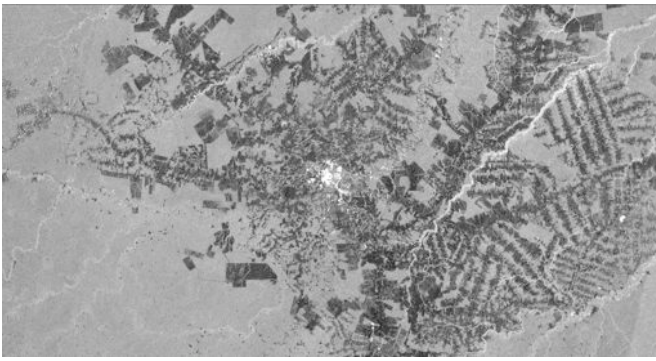


Figure 12. Rio Branco from mosaic of average of ScanSAR images.

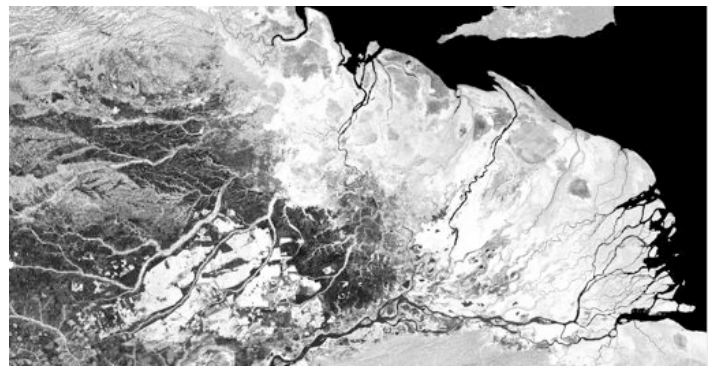


Figure 15: Orinoco River from mosaic of average of ScanSAR images.

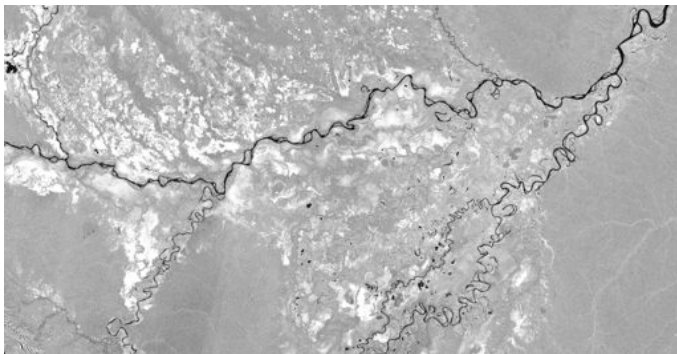


Figure 13. Palm Swamps in Peru from mosaic of average of ScanSAR images.

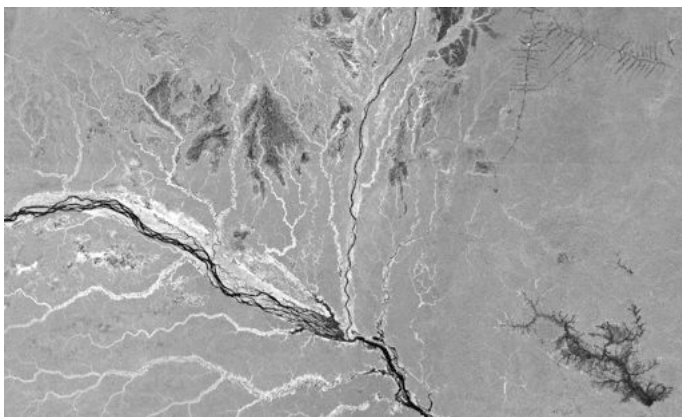


Figure 14. Rio Negro from mosaic of average of ScanSAR images.

The mosaic of the average of ScanSAR images is a time averaged image and not necessary straightforward to interpret, however, it clearly delineates areas of interest for studying wetland dynamics. For quantitative time series analysis of wetland dynamics, the single cycle mosaics must be used. For instance, figure 16 shows a color composite of a wetland area near Guayaramer, Boliva (-12.7 degrees Latitude, -65.2 degrees Longitude), in which red is the cycle 9\_10 mosaic, green is the cycle 11\_12 mosaic, and blue is the cycle 13\_14 mosaic. This image illustrates the sensitivity of the ALOS ScanSAR imagery to change in inundation, and the separability of various land cover types from these signatures.

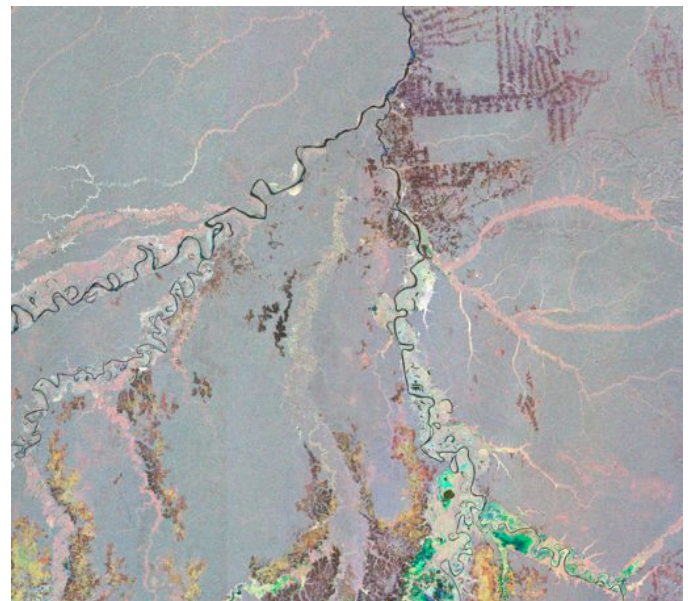


Figure 16. This image is about 200 m pixel spacing, and is a color composite of three ScanSAR mosaics (which red is the cycle 9\_10 mosaic, green is the cycle 11\_12 mosaic, and blue is the cycle 13\_14 mosaic). The image is centered on GUAYARAMER, Bolivia (-11.3 degrees Latitude, -65.6 degrees Longitude).

One objective of this work is to compare wetland classifications generated from high resolution ALOS PALSAR data with that generated from much lower resolution (but much shorter orbit repeat intervals) passive spaceborne sensors such as AMSR-E. Therefore, using the illustrative but not definitive thresholding algorithm shown in figures 7 and 8, the fractional inundation was estimated to demonstrate how correspondences between these data products will be assessed. The fractional inundation is simply the fraction of the pixels within a region that are classified as either open water or inundated vegetation. For this example, we separately calculated the fraction of open water (figure 17), and the fraction of inundated vegetation (figure 18), for each one degree by one degree cell within UTM grid-zone tile 19M. As can be seen, the fraction of open water, as expected, does not change as much as the fraction of inundated vegetation.



Figure 17a) Fractional open water May-June 2007, tile 19M. The fraction of open water varies from 0 (green) to 5 %. (yellow)



Figure 17b) Fractional open water July 2007, tile 19M. The fraction of open water varies from 0 (green) to 5 %. (yellow)

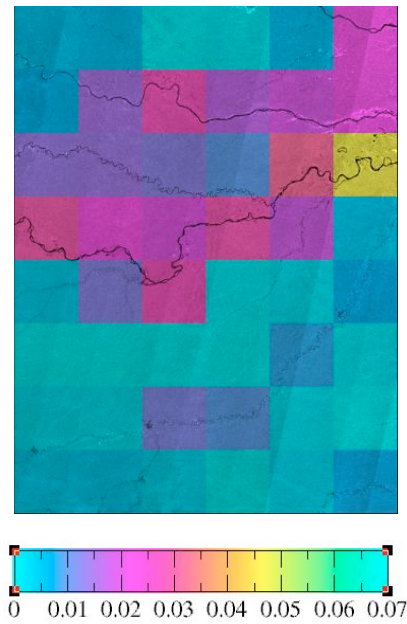


Figure 17c) Fractional open water for Aug-Sept 2007, tile 19M. The fraction of open water varies from 0 (green) to 5 %. (yellow)

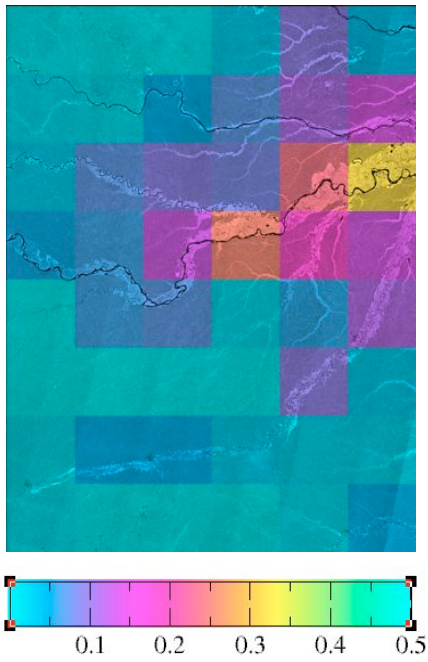


Figure 18a) Fractional inundated vegetation for May-June 2007, tile 19M, varies from 0 (green) to 30 % (yellow).

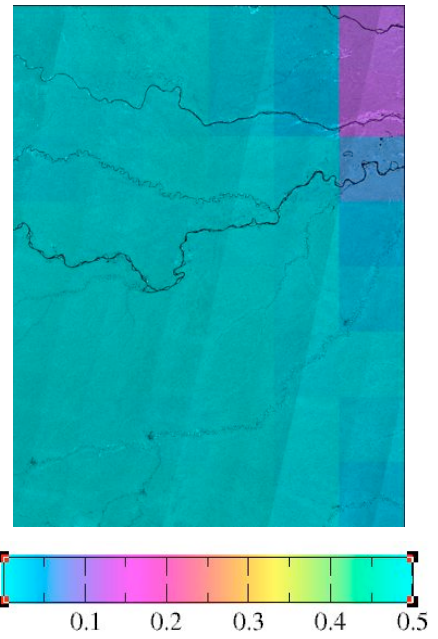


Figure 18c) Fractional inundated vegetation for Aug-Sept 2007, tile 19M, varies from 0 (green) to 30 % (yellow).

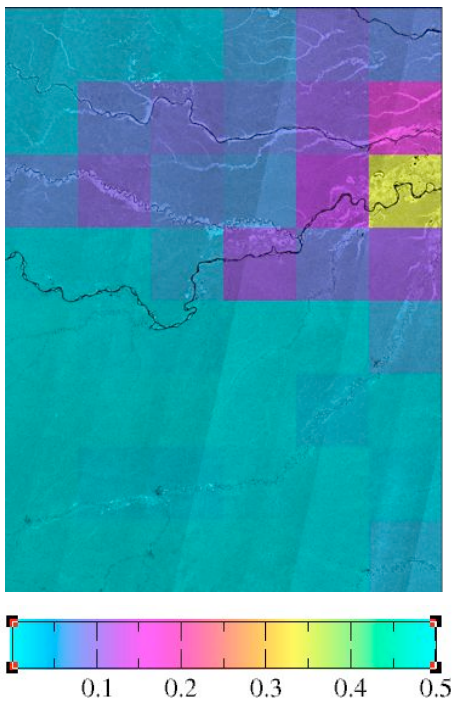


Figure 18b) Fractional inundated vegetation for July 2007, tile 19M, varies from 0 (green) to 30 % (yellow).

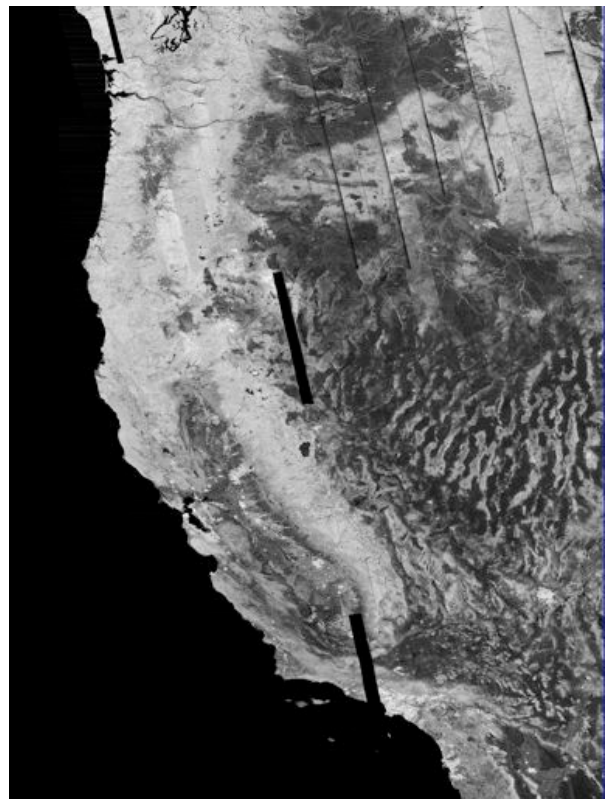


Figure 19a) Four UTM grid-zone tiles covering the Western US, HH Polarization

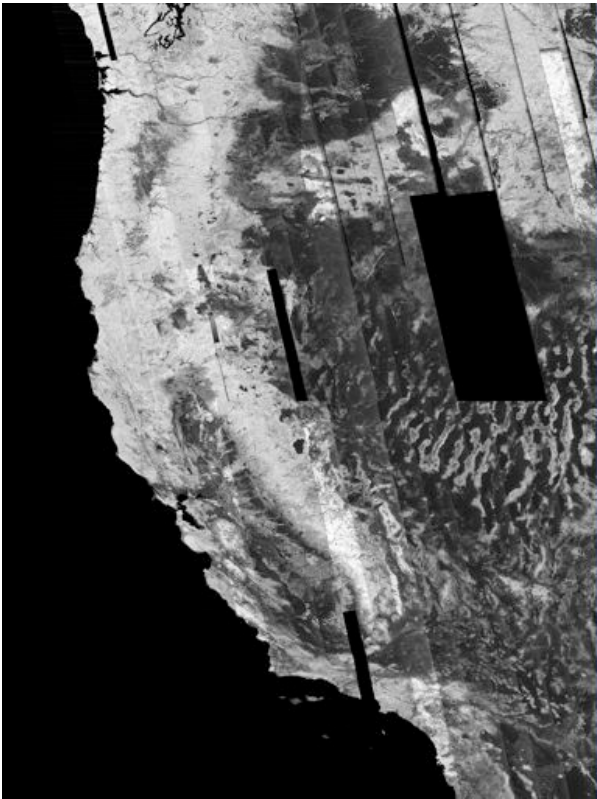


Figure 19b) Four UTM grid –zone tiles covering the Western US, HV Polarization

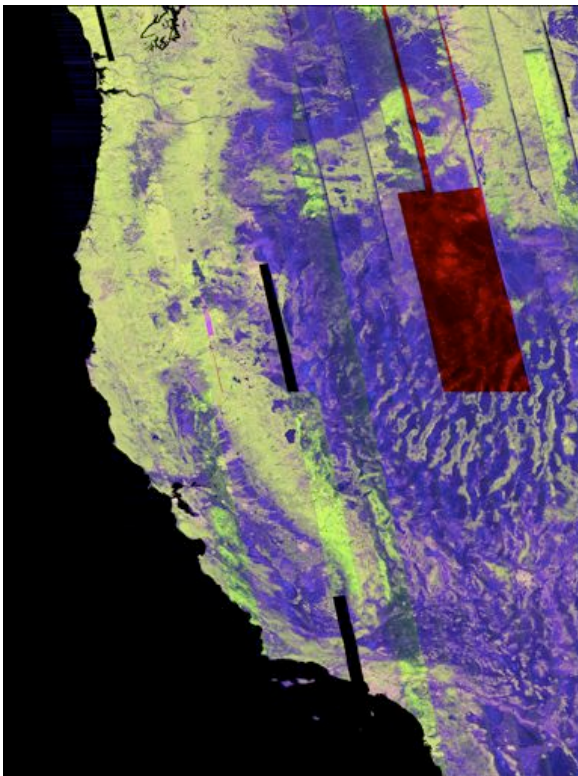


Figure 19c) Four UTM grid –zone tiles covering the Western US, color composite (HH: red, HV: green, HH/HV: blue). Gaps and calibration errors are clearly visible.

For dual polarization mosaics, the mosaics are posted at a pixel spacing of 2 arcsecond, or approximately 60 meters. Figure 19 shows an FBD dual polarization mosaic for UTM grid-zone tiles 10S 10T 11S and 11T covering the western United States. The dual polarization data will be used by this wetlands mapping activity to discriminate the underlying vegetation structure of the wetland areas.

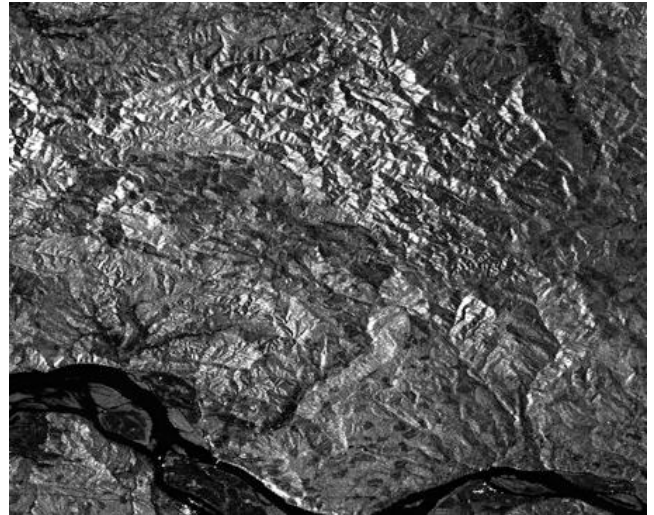


Figure 20a) HH image (from mosaic shown in figure 19) without radiometric terrain correction.

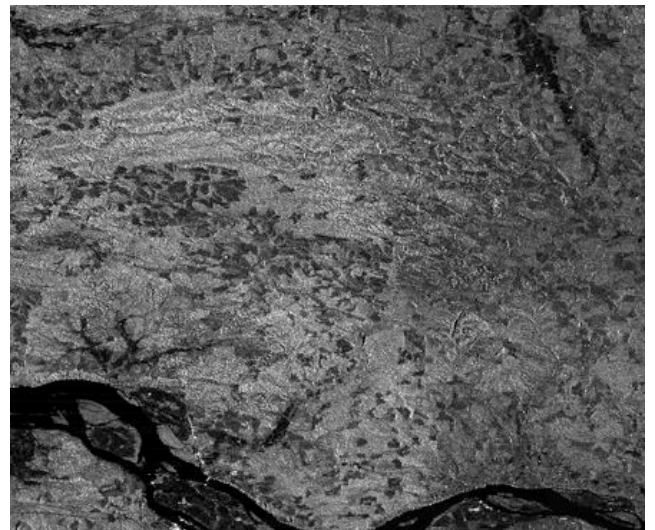


Figure 20b) HH image (from mosaic shown in figure 19) with radiometric terrain correction.

A subset of data from the Northwest US shown in figure 19 illustrates the utility of radiometric terrain correction for identification of land cover types other than those related to wetlands. Figure 20 shows a mountainous region before and after terrain correction. As can be seen if examined at full

resolution, while the terrain correction does not remove all terrain effects from the imagery, it does substantially improve the utility of the image mosaics for indicating different land cover types, such as clearings from undisturbed forest.

This work has occurred during phase 2 of the KC initiative, and is still ongoing as calibration improvements are tested and implemented, gaps in processing and ortho-rectification are filled, and further coverage is undertaken. Validated wetlands products are under development as separate components of this task.

#### ACKNOWLEDGEMENTS

This paper was partially written at the Jet Propulsion Laboratory, California Institute of Technology, under contract with the National Aeronautics and Space Administration. This work has been undertaken in part within the framework of the JAXA Kyoto & Carbon Initiative. ALOS PALSAR data have been provided by JAXA EORC. Copyright 2009 California Institute of Technology. Government sponsorship acknowledged.

#### REFERENCES

- [1] M. Shimada, "PALSAR and Calibration update". *11<sup>th</sup> ALOS K&C Science Team meeting (KC#11)*, Tsukuba, Japan, Jan. 13-16, 2009. [Online] Available: [http://www.eorc.jaxa.jp/ALOS/kyoto/jan2009\\_kc11/pdf/090113/shimada\\_calval\\_up\\_090113.pdf](http://www.eorc.jaxa.jp/ALOS/kyoto/jan2009_kc11/pdf/090113/shimada_calval_up_090113.pdf)
- [2] A. Rosenqvist, M. Shimada, R. Lucas, J. Lowry, P. Pailou, B. Chapman [eds.], "The ALOS Kyoto & Carbon Initiative, Science Plan (v.3.1)," JAXA EORC, March, 2008. [Online] Available: [http://www.eorc.jaxa.jp/ALOS/kyoto/KC-Science-Plan\\_v3.1.pdf](http://www.eorc.jaxa.jp/ALOS/kyoto/KC-Science-Plan_v3.1.pdf)
- [3] ALOS Kyoto & Carbon Initiative home page: [http://www.eorc.jaxa.jp/ALOS/kyoto/kyoto\\_index.htm](http://www.eorc.jaxa.jp/ALOS/kyoto/kyoto_index.htm)
- [4] K&C Wiki site. <http://www.ies.aber.ac.uk/en/subsites/the-alos-kyoto-amp-carbon-initiative>
- [5] K&C Wiki site. <http://www.ies.aber.ac.uk/en/subsites/the-alos-kyoto-amp-carbon-initiative/latest-news>
- [6] Rosenqvist A., Shimada M., Ito N. and Watanabe M. "ALOS PALSAR: A pathfinder mission for global-scale monitoring of the environment," *IEEE Trans. Geosci. Remote Sens*, vol. 45, no. 11, pp. 3307-3316, 2007.
- [7] C. Werner, U. Wegmüller, T. Strozzi, and A. Wiesmann, "Gamma SAR and interferometric processing software," in *Proc. ERS-ENVISAT Symp.*, Gothenburg, Sweden, Oct. 16–20, 2000.
- [8] McDonald, K.C., Chapman, B., Podest, E., Jimenez, A, "Assessment of a Near-Global 30-Meter Resolution DEM Derived from the Publicly Available SRTM Data Set for Use in Orthorectification of Satellite SAR Imagery," *AGU*, FALL 2007.
- [9] SRTM 90 m Digital Elevation Data from CGIAR-SCI <http://srtm.csi.cgiar.org/>
- [10] UTM Grid Zones of the World, compiled by Alan Morton, <http://www.dmap.co.uk/utmworld.htm>
- [11] Siqueira, P., Hensley, S., Shaffer, S., Hess, L., McGarragh, G., Chapman, B., Holt, J., & Freeman, A. (2000). A continental scale mosaic of the Amazon basin using JERS-1 SAR. *IEEE Transactions on Geoscience and Remote Sensing*, 30(6), 2638–2644.
- [12] Lucas, R.; Armston, J.; Fairfax, R.; Fensham, R.; Accad, A.; Carreiras, J.; Kelley, J.; Bunting, P.; Clewley, D.; Bray, S.; Metcalfe, D.; Dwyer, J.; Bowen, M.; Eyre, T.; Laidlaw, M.; Shimada, M.; , "An Evaluation of the ALOS PALSAR L-Band Backscatter—Above Ground Biomass Relationship Queensland, Australia: Impacts of Surface Moisture Condition and Vegetation Structure," *Selected Topics in Applied Earth Observations and Remote Sensing, IEEE Journal of* , vol.3, no.4, pp.576-593, Dec. 2010
- [13] NASA Ames Advanced Supercomputing Division, <http://www.nas.nasa.gov/>



**Bruce Chapman** is a senior member of the technical staff at the Jet Propulsion Laboratory, California Institute of Technology, in Pasadena, California. He received his Bachelor of Arts degree in Physics and Astronomy from the University of California, Berkeley in 1981, and his Ph.D. in Earth, Atmospheric and Planetary Sciences from the Massachusetts Institute of Technology in 1986. He is currently an investigator in NASA's Terrestrial Ecology, Space Archaeology, and MEASUREs programs, studying forest structure measurements using Synthetic Aperture Radar, and the utilization of airborne Synthetic Aperture Radar in Mayan Archaeology regions in Central America; as well as participating in the production of an Earth Science Data Record for Inundated Wetlands using ALOS SAR data.